Inorg. Chem. **2004**, *43*, 3882–3893

Two- and Three-Dimensional Cadmium–Organic Frameworks with Trimesic Acid and 4,4′-Trimethylenedipyridine

Filipe A. Almeida Paz and Jacek Klinowski*

Department of Chemistry, University of Cambridge, Lensfield Road, Cambridge CB2 1EW, U.K.

Received April 12, 2004

Three novel cadmium–organic frameworks built-up from 1,3,5-benzenetricarboxylate anions (H_XBTC^{x-3}) and 4,4′-trimethylenedipyridine (TMD) have been hydrothermally synthesized, and characterized using single-crystal X-ray diffraction, thermoanalytical measurements, elemental analysis, and IR and Raman spectroscopies: $[Cd(HBTC)(TMD)_2]\cdot 8.5H_2O$ (**I**), $[Cd(HBTC)(TMD)(H_2O)]\cdot 4.5H_2O$ (**II**), and $[Cd_2(BTC)(TMD)_2(NO_3)]\cdot 3H_2O$ (**III**), with structures **I** and **II** being isolated as a mixture of crystals. Structure **I** contains an undulating infinite two-dimensional $[Cd(HBTC)(TMD)_2]$ framework, with a (4,4) topology and rectangular pores, ca. 3.4 × 11.0 Å in cross-section, distributed in a herringbone manner. The crystal structure of **I** is obtained by parallel packing of this 2D framework in an [ABAB···] fashion. Compound **II** has a porous 3D diamondoid framework with channels running in several directions of the unit cell, which allows 2-fold interpenetration to occur. The most prominent channels are distributed in a brick-wall fashion along the *c* axis and have a cross-section of ca. 3.2 × 13.2 Å. Structure **III** can be seen as the three-dimensional assembly of binuclear secondary building units (SBU), which leads to a compact, neutral, and coordinatively bonded eight-connected framework, $[Cd_2(BTC)(TMD)_2(NO_3)]$, exhibiting an unusual 3^64^{22} topology. The increased flexibility of the TMD ligands (brought about by the three methylene groups between the two 4-pyridyl rings) can lead, for the same reactive system, to a large variety of crystal architectures.

Introduction

The construction of large networks, with predictable topologies and properties controlled by the chemical nature of the components, and their interactions in the solid state, is one the main goals of crystal engineers working on the synthesis of purely organic molecular crystals and metal–organic frameworks (MOFs).[1−3] The term *crystal engineering* was first used by Schmidt[4] and implies that, under specific conditions, the chemical components of a given reactive mixture self-assemble via a series of molecular recognition events. However, although all crystal structures are formed by the same driving forces (molecular recognition events in solution, close packing, and space filling),[5] it appears that the answer to the question, "Are crystal structures predictable?" recently asked by Dunitz,[6] is "No".

Much work has been devoted to the design, synthesis, and structural characterization of novel multidimensional MOFs,[1,2,7] with the increasing volume of research being reflected in the exponential growth of the number of structures reported over the past few years. These structures are essentially assembled by very strong and highly directional coordinative interactions (several hundreds of kJ mol^{-1})[8] between metal centers and multitopic organic ligands (with one or more donor atoms), thus combining properties of both purely organic and inorganic compounds. Furthermore, the motiva-

* Author to whom correspondence should be addressed. Professor Jacek Klinowski, Department of Chemistry, University of Cambridge, Lensfield Road, Cambridge CB2 1EW, U.K. E-mail: jk18@cam.ac.uk. Telephone: +(44)-01223-33 65 09. Fax: +(44)-01223-33 63 62.

(1) Moulton, B.; Zaworotko, M. J. *Chem. Rev.* **2001**, *101*, 1629.
(2) Zaworotko, M. J. *Chem. Commun.* **2001**, 1; Batten, S. R.; Robson, R. *Angew. Chem., Int. Ed.* **1998**, *37*, 1461; Kitagawa, S.; Kondo, M. *Bull. Chem. Soc. Jpn.* **1998**, *71*, 1739; Desiraju, G. R. *Angew. Chem., Int. Ed. Engl.* **1995**, *34*, 2311.
(3) Desiraju, G. R. *Crystal Engineering: The Design of Organic Solids*; Elsevier: Amsterdam, 1989; Jones, W. *Organic Molecular Solids: Properties and Applications*; CRC Press: New York, 1997; Bond, A. D.; Jones, W. In *Supramolecular Organization and Materials Design*; Jones, W., Rao, C. N. R., Eds.; Cambridge University Press: Cambridge, 2002, p 391.
(4) Schmidt, G. M. *J. Pure Appl. Chem.* **1971**, *27*, 647.
(5) Aitipamula, S.; Thallapally, P. K.; Thaimattam, R.; Jaskolski, M.; Desiraju, G. R. *Org. Lett.* **2002**, *4*, 921.
(6) Dunitz, J. D. *Chem. Commun.* **2003**, 545.
(7) Janiak, C. *Angew. Chem., Int. Ed. Engl.* **1997**, *36*, 1431; Janiak, C. *Dalton Trans.* **2003**, 2781; Yaghi, O. M.; Li, H. L.; Davis, C.; Richardson, D.; Groy, T. L. *Acc. Chem. Res.* **1998**, *31*, 474.
(8) Coe, S.; Kane, J. J.; Nguyen, T. L.; Toledo, L. M.; Wininger, E.; Fowler, F. W.; Lauher, J. W. *J. Am. Chem. Soc.* **1997**, *119*, 86; Braga, D.; Angeloni, A.; Maini, L.; Gotz, A. W.; Grepioni, F. *New J. Chem.* **1999**, *23*, 17.

10.1021/ic049523o CCC: $27.50
Published on Web 05/27/2004

Scheme 1

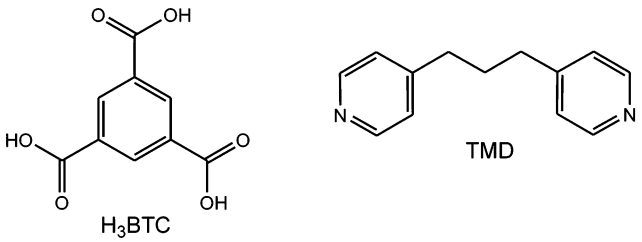

tion behind such research lies in the large variety of peculiar architectures, together with the various potential applications of these compounds as functional materials (e.g., porosity allied with guest exchange, catalysis, gas storage, photoluminescence, nonlinear optical properties, chirality, clathration abilites, and magnetic properties).[9,10]

Rodlike *N*,*N*′-donor ligands, such as the traditionally used 4,4′-bipyridine (4,4′-bpy), and molecules containing two or more *exo*-carboxylic acid groups able to coordinate to several metal centers in various modes, have been systematically used for the synthesis of multidimensional MOFs. In particular, 1,3,5-benzenetricarboxylic acid (H_3BTC, also known as trimesic acid; Scheme 1) is a rigid planar molecule containing three *exo*-carboxylic acid groups arranged symmetrically around the benzene ring, thus forming a flat trigonal ligand, which can be used as a building block. H_3BTC has been extensively used in the synthesis of multidimensional MOFs containing a large variety of metal centers.[10−12] When chemical aggregates, such as methylene groups, are selectively introduced between the two 4-pyridyl rings of 4,4-bpy, the resulting ligand acquires variable flexibility and functionality, which can direct interesting framework properties (dimensionality, void space, degree of interpenetration, and topology). In this context, 1,2-bis(4-pyridyl)ethane (BPE)[13] and 4,4′-trimethylenedipyridine (TMD)[14,15] (Scheme 1) are good candidates for studying the effect of their flexibility on the structural properties of MOFs.

Following our interest in the hydrothermal synthesis of novel organic crystals[16,17] and MOFs (in particular those containing Cd^{2+} cations),[13,18−20] we wish to report three novel two-dimensional (2D) and three-dimensional (3D) cadmium−organic frameworks simultaneously incorporating H_xBTC^{x-3} residues and TMD ligands: $[Cd(HBTC)(TMD)_2]\cdot 8.5H_2O$ (**I**) (2D framework with (4,4) topology), $[Cd(HBTC)(TMD)(H_2O)]\cdot 4.5H_2O$ (**II**) (3D 2-fold interpenetrated diamondoid frameworks), and $[Cd_2(BTC)(TMD)_2(NO_3)]\cdot 3H_2O$ (**III**) (a compact eight-connected 3D modular structure with an unusual 3^64^{22} topology). The increased flexibility of TMD, when compared to that of BPE,[13] leads to a larger variety of possible structures (which Moulton and Zaworotko call

(9) Eddaoudi, M.; Li, H. L.; Yaghi, O. M. *J. Am. Chem. Soc.* **2000**, *122*, 1391; Li, H.; Eddaoudi, M.; Groy, T. L.; Yaghi, O. M. *J. Am. Chem. Soc.* **1998**, *120*, 8571; Reineke, T. M.; Eddaoudi, M.; Fehr, M.; Kelley, D.; Yaghi, O. M. *J. Am. Chem. Soc.* **1999**, *121*, 1651; Rosi, N. L.; Eckert, J.; Eddaoudi, M.; Vodak, D. T.; Kim, J.; O'Keeffe, M.; Yaghi, O. M. *Science* **2003**, *300*, 1127; Kitaura, R.; Seki, K.; Akiyama, G.; Kitagawa, S. *Angew. Chem., Int. Ed.* **2003**, *42*, 428; Tong, M. L.; Shi, J. X.; Chen, X. M. *New J. Chem.* **2002**, *26*, 814; Lin, W. B.; Ma, L.; Evans, O. R. *Chem. Commun.* **2000**, 2263; Matouzenko, G. S.; Molnar, G.; Brefuel, N.; Perrin, M.; Bousseksou, A.; Borshch, S. A. *Chem. Mater.* **2003**, *15*, 550; Niel, V.; Thompson, A. L.; Munoz, M. C.; Galet, A.; Goeta, A. S. E.; Real, J. A. *Angew. Chem., Int. Ed.* **2003**, *42*, 3760; Evans, O. R.; Ngo, H. L.; Lin, W. *J. Am. Chem. Soc.* **2001**, *123*, 10395; Seo, J. S.; Whang, D.; Lee, H.; Jun, S. I.; Oh, J.; Jeon, Y. J.; Kim, K. *Nature* **2000**, *404*, 982; Fujita, M.; Kwon, Y. J.; Washizu, S.; Ogura, K. *J. Am. Chem. Soc.* **1994**, *116*, 1151.

(10) Yaghi, O. M.; Li, G. M.; Li, H. L. *Nature* **1995**, *378*, 703; Yaghi, O. M.; Li, H. L.; Groy, T. L. *J. Am. Chem. Soc.* **1996**, *118*, 9096.

(11) Plater, M. J.; Roberts, A. J.; Marr, J.; Lachowski, E. E.; Howie, R. A. *J. Chem. Soc.-Dalton Trans.* **1998**, 797; Platers, M. J.; Howie, R. A.; Roberts, A. J. *Chem. Commun.* **1997**, 893; Dai, J. C.; Wu, X. T.; Fu, Z. Y.; Cui, C. P.; Hu, S. M.; Du, W. X.; Wu, L. M.; Zhang, H. H.; Sun, R. O. *Inorg. Chem.* **2002**, *41*, 1391; Skakle, J. M. S.; Foreman, M. R. S.; Plater, M. J.; Griffin, C. *Acta Crystallogr., Sect. E* **2001**, *57*, M85; Dimos, A.; Michaelides, A.; Skoulika, S. *Chem. Mater.* **2000**, *12*, 3256; Livage, C.; Guillou, N.; Marrot, J.; Ferey, G. *Chem. Mater.* **2001**, *13*, 4387; Guillou, N.; Livage, C.; Marrot, J.; Ferey, G. *Acta Crystallogr., Sect. C: Cryst. Struct. Commun.* **2000**, *56*, 1427; Chatterjee, S.; Pedireddi, V. R.; Ranganathan, A.; Rao, C. N. R. *J. Mol. Struct.* **2000**, *520*, 107; Plater, M. J.; Foreman, M. R. S.; Howie, R. A.; Skakle, J. M. S.; Coronado, E.; Gomez-Garcia, C. J.; Gelbrich, T.; Hursthouse, M. B. *Inorg. Chim. Acta* **2001**, *319*, 159; Plater, M. J.; Foreman, M. R. S.; Coronado, E.; Gomez-Garcia, C. J.; Slawin, A. M. Z. *J. Chem. Soc., Dalton Trans.* **1999**, 4209; Ko, J. W.; Min, K. S.; Suh, M. P. *Inorg. Chem.* **2002**, *41*, 2151; Cheng, D. P.; Khan, M. A.; Houser, R. P. *Inorg. Chem.* **2001**, *40*, 6858; Chui, S. S. Y.; Lo, S. M. F.; Charmant, J. P. H.; Orpen, A. G.; Williams, I. D. *Science* **1999**, *283*, 1148; Chui, S. S. Y.; Siu, A.; Williams, I. D. *Acta Crystallogr., Sect. C: Cryst. Struct. Commun.* **1999**, *55*, 194; Pech, R.; Pickardt, J. *Acta Crystallogr., Sect. C: Cryst. Struct. Commun.* **1988**, *44*, 992; Daiguebonne, C.; Guilloa, O.; Gerault, Y.; Lecerf, A.; Boubekeur, K. *Inorg. Chim. Acta* **1999**, *284*, 139; Daiguebonne, C.; Guillou, O.; Boubekeur, K. *Inorg. Chim. Acta* **2000**, *304*, 161; Riou-Cavellec, M.; Albinet, C.; Greneche, J. M.; Ferey, G. *J. Mater. Chem.* **2001**, *11*, 3166; Prior, T. J.; Rosseinsky, M. J. *Chem. Commun.* **2001**, 495; Prior, T. J.; Rosseinsky, M. J. *Chem. Commun.* **2001**, 1222; Choi, K. Y.; Chun, K. M.; Suh, I. H. *Polyhedron* **2001**, *20*, 57; Kepert, C. J.; Prior, T. J.; Rosseinsky, M. J. *J. Am. Chem. Soc.* **2000**, *122*, 5158; Kepert, C. J.; Prior, T. J.; Rosseinsky, M. J. *J. Solid State Chem.* **2000**, *152*, 261; Kepert, C. J.; Rosseinsky, M. J. *Chem. Commun.* **1998**, 31; Choi, H. J.; Suh, M. P. *J. Am. Chem. Soc.* **1998**, *120*, 10622; Foreman, M.; Gelbrich, T.; Hursthouse, M. B.; Plater, M. J. *Inorg. Chem. Commun.* **2000**, *3*, 234; Sobota, P.; Utko, J.; Lis, T. *J. Organomet. Chem.* **1993**, *447*, 213; Yaghi, O. M.; Li, G. M.; Li, H. L. *Chem. Mater.* **1997**, *9*, 1074; Smith, G.; Reddy, A. N.; Byriel, K. A.; Kennard, C. H. L. *J. Chem. Soc., Dalton Trans.* **1995**, 3565; Prior, T. J.; Rosseinsky, M. J. *Inorg. Chem.* **2003**, *42*, 1564; Prior, T. J.; Bradshaw, D.; Teat, S. J.; Rosseinsky, M. J. *Chem. Commun.* **2003**, *500*; Chen, W.; Wang, J. Y.; Chen, C.; Yue, Q.; Yuan, H. M.; Chen, J. S.; Wang, S. N. *Inorg. Chem.* **2003**, *42*, 944; Wu, G.; Shi, X.; Fang, Q. R.; Tian, G.; Wang, L. F.; Zhu, G. S.; Addison, A. W.; Wei, Y.; Qiu, S. L. *Inorg. Chem. Commun.* **2003**, *6*, 402; Yang, X. J.; Wu, B.; Sun, W. H.; Janiak, C. *Inorg. Chim. Acta* **2003**, *343*, 366.

(12) Yaghi, O. M.; Davis, C. E.; Li, G. M.; Li, H. L. *J. Am. Chem. Soc.* **1997**, *119*, 2861.

(13) Paz, F. A. A.; Klinowski, J. *Inorg. Chem.* **2004**, submitted.

(14) Plater, M. J.; Foreman, M. R. S.; Howie, R. A.; Skakle, J. M. S. *Inorg. Chim. Acta* **2001**, *318*, 175; Dong, Y. B.; Smith, M. D.; Layland, R. C.; zur Loye, H. C. *Inorg. Chem.* **1999**, *38*, 5027; Carlucci, L.; Ciani, G.; Moret, M.; Proserpio, D. M.; Rizzato, S. *Chem. Mater.* **2002**, *14*, 12; Tabellion, F. M.; Seidel, S. R.; Arif, A. M.; Stang, P. J. *J. Am. Chem. Soc.* **2001**, *123*, 11982; Pan, L.; Woodlock, E. B.; Wang, X. T.; Lam, K. C.; Rheingold, A. L. *Chem. Commun.* **2001**, 1762; Fu, Z. Y.; Lin, P.; Du, W. X.; Chen, L.; Cui, C. P.; Zhang, W. J.; Wu, X. T. *Polyhedron* **2001**, *20*, 1925; Tabellion, F. M.; Seidel, S. R.; Arif, A. M.; Stang, P. J. *Angew. Chem., Int. Ed.* **2001**, *40*, 1529; Plater, M. J.; Foreman, M. R. S.; Gelbrich, T.; Hursthouse, M. B. *Inorg. Chim. Acta* **2001**, *318*, 171; Carlucci, L.; Ciani, G.; Moret, M.; Proserpio, D. M.; Rizzato, S. *Angew. Chem., Int. Ed.* **2000**, *39*, 1506; Batten, S. R.; Jeffery, J. C.; Ward, M. D. *Inorg. Chim. Acta* **1999**, *292*, 231; Mao, J. G.; Zhang, H. J.; Ni, J. Z.; Wang, S. B.; Mak, T. C. W. *Polyhedron* **1999**, *18*, 1519.

(15) Carlucci, L.; Ciani, G.; Proserpio, D. M.; Rizzato, S. *CrystEngComm* **2002**, 121; Plater, M. J.; Foreman, M. R. S.; Gelbrich, T.; Coles, S. J.; Hursthouse, M. B. *J. Chem. Soc., Dalton Trans.* **2000**, 3065.

(16) Paz, F. A. A.; Bond, A. D.; Khimyak, Y. Z.; Klinowski, J. *New J. Chem.* **2002**, *26*, 381.

(17) Paz, F. A. A.; Klinowski, J. *CrystEngComm* **2003**, *5*, 238.

Table 1. Crystal Data and Structure Refinement Information for Compounds **I**, **II**, and **III**

	I	II	III
formula	$CdC_{35}H_{49}N_4O_{14.50}$	$CdC_{22}H_{29}N_2O_{11.50}$	$Cd_2C_{35}H_{37}N_5O_{12}$
fw	870.18	617.87	944.50
cryst syst	monoclinic	monoclinic	monoclinic
space group	$P2_1/n$	$C2/c$	$P2_1/n$
a/Å	10.6077(2)	13.9970(10)	9.8976(2)
b/Å	20.9159(5)	20.103(2)	14.5822(4)
c/Å	18.3970(4)	17.460(2)	26.5732(7)
β/°	105.0490(10)	100.201(5)	91.930(1)
vol/Å^3	3941.75(15)	4835.3(8)	3833.10(17)
Z	4	8	4
D_c/g cm^{-3}	1.466	1.698	1.637
μ(Mo Kα)/mm^{-1}	0.625	0.970	1.176
cryst size/mm	0.15 × 0.05 × 0.05	0.16 × 0.12 × 0.05	0.07 × 0.05 × 0.02
cryst type	colorless needles	colorless blocks	colorless blocks
θ range	3.53 to 27.48°	3.59 to 25.02°	3.54 to 27.48°
index ranges	$-13 \le h \le 13$	$-16 \le h \le 15$	$-12 \le h \le 12$
	$-26 \le k \le 27$	$-22 \le k \le 23$	$-18 \le k \le 18$
	$-23 \le l \le 23$	$-20 \le l \le 20$	$-25 \le l \le 34$
rflns collected	35843	17254	21941
independent reflns	8965 (R_{int} = 0.0605)	4026 (R_{int} = 0.0697)	8730 (R_{int} = 0.0619)
final R indices [$I > 2\sigma(I)$]	R1 = 0.0428, wR2 = 0.1016	R1 = 0.0992, wR2 = 0.2301	R1 = 0.0928, wR2 = 0.1959
final R indices (all data)	R1 = 0.0664, wR2 = 0.1141	R1 = 0.1272, wR2 = 0.2445	R1 = 0.1401, wR2 = 0.2103
largest diff peak and hole	1.287 and −0.939 eÅ^{-3}	1.697 and −1.304 eÅ^{-3}	2.831 and −1.306 eÅ^{-3}

supramolecular isomerism),[1] and also to significantly less crystalline materials.

Results and Discussion

Crystal Structures of [Cd(HBTC)(TMD)$_2$]·8.5(H$_2$O) (I) and [Cd(HBTC)(TMD)(H$_2$O)]·4.5(H$_2$O) (II). The hydrothermal reaction, under mild conditions, between 1,3,5-benzenetricarboxylic acid (H_3BTC, also known as trimesic acid) and 4,4′-trimethylenedipyridine (TMD; see Scheme 1) resulted in the formation of a white compact solid, capable of containing all the solvent used during the synthesis. A microscopic inspection showed a mixture of two different types of very small crystals. Single crystals suitable for X-ray diffraction could only be obtained by leaving the content of the autoclave undisturbed for 10 weeks at ambient temperature, which allowed the crystals to grow very slowly at the expense of the starting materials in the mother liquor.[21] Long needles and small blocks (see Supporting Information, Figure S1a,b) were manually harvested and formulated as [Cd(HBTC)(TMD)$_2$]·8.5H$_2$O (**I**) and [Cd(HBTC)(TMD)(H$_2$O)]·4.5H$_2$O (**II**), respectively, by single-crystal X-ray diffraction (Table 1).

Both structures have only one repeating metallic structural motif, with each crystallographically unique Cd^{2+} metal center in a heptacoordinated and distorted pentagonal bipyramidal coordination fashion (Figures 1 and 2; Tables 2 and 3): in **I**, the Cd^{2+} is coordinated to two $HBTC^{2-}$ and three TMD ligands, {CdO_4N_3} (Figure 1 and Table 2), while in **II** the coordination environment is described by {CdO_5N_2} due to the coordination to two $HBTC^{2-}$, two TMD, and one water molecule (Figure 2 and Table 3). The classification of the coordination environments as distorted pentagonal bipyramids is based upon the fact that the Cd−O bonds for the coordinated carboxylate groups are statistically different. This is particularly evident for the C(17) and C(19) carboxylate groups in **II** [e.g., Cd(1)−O(171) 2.484(9) Å versus Cd(1)−O(172) 2.322(8) Å; see Table 3]. The average Cd−O and Cd−N bond lengths are 2.45/2.41 and 2.34/2.33 Å (**I**/**II**), respectively. While virtually identical to the values reported for other MOFs,[22] these bond lengths are slightly larger than in the structure containing 1,2-Bis(4-pyridyl)-ethane (BPE), [$Cd_{1.5}$(BTC)(BPE)(H$_2$O)$_2$]·H$_2$O.[13] This is attributed to the increase in the coordination number of the

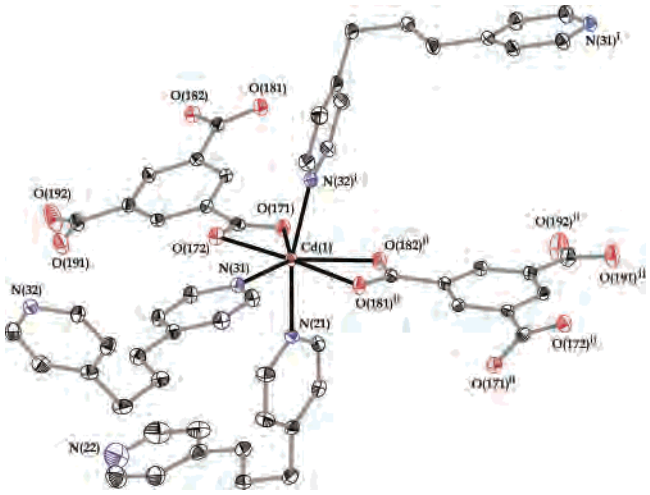

Figure 1. Distorted octahedral coordination environment for the Cd^{2+} metal center in **I**. Hydrogen atoms have been omitted for clarity, and thermal ellipsoids are drawn at the 30% probability level. For bond lengths (in Å) and angles (in degrees) see Table 2. Symmetry codes used to generate equivalent atoms: (i) 1/2 − x, 1/2 + y, 1/2 − z; (ii) 1/2 + x, 1/2 − y, 1/2 + z.

(18) Paz, F. A. A.; Bond, A. D.; Khimyak, Y. Z.; Klinowski, J. *Acta Crystallogr., Sect. E* **2002**, *58*, M730; Paz, F. A. A.; Bond, A. D.; Khimyak, Y. Z.; Klinowski, J. *Acta Crystallogr., Sect. C: Cryst. Struct. Commun.* **2002**, *58*, M608; Paz, F. A. A.; Bond, A. D.; Khimyak, Y. Z.; Klinowski, J. *Acta Crystallogr., Sect. E* **2002**, *58*, M691; Paz, F. A. A.; Klinowski, J. *J. Phys. Org. Chem.* **2003**, *16*, 772; Paz, F. A. A.; Klinowski, J. *Chem. Commun.* **2003**, 1484; Paz, F. A. A.; Shi, F.-N.; Klinowski, J.; Rocha, J.; Trindade, T. *Eur. J. Inorg. Chem.* **2003**, submitted.
(19) Paz, F. A. A.; Khimyak, Y. Z.; Bond, A. D.; Rocha, J.; Klinowski, J. *Eur. J. Inorg. Chem.* **2002**, 2823.
(20) Paz, F. A. A.; Klinowski, J. *J. Sol. State Chem.* **2004**, in press.
(21) Markov, I. V. *Crystal Growth for Beginners: Fundamentals of Nucleation, Crystal Growth and Epitaxy*; 2nd ed.; World Scientific Publishing Co. Pte. Ltd.: Singapore, 2003.

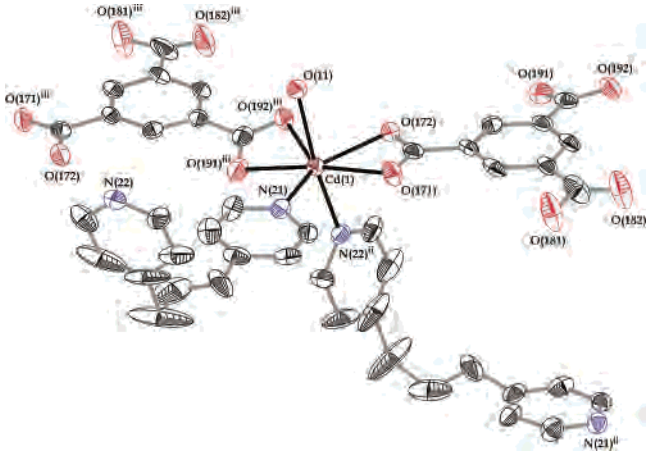

Figure 2. Distorted octahedral coordination environment for the Cd^{2+} metal center in **II**. Hydrogen atoms have been omitted for clarity, and thermal ellipsoids are drawn at the 30% probability level. For bond lengths (in Å) and angles (in degrees) see Table 3. Symmetry codes used to generate equivalent atoms: (ii) 1/2 + *x*, 1/2 − *y*, 1/2 + *z*; (iii) *x*, −*y*, *z* − 1/2.

Table 2. Selected Bond Lengths (in Å) and Angles (in degrees) for **I**[a]

Cd(1)−O(171)	2.481(2)	O(171)−Cd(1)−O(172)	53.88(7)
Cd(1)−O(172)	2.399(2)	O(172)−Cd(1)−N(31)	83.04(8)
Cd(1)−N(21)	2.336(2)	N(31)−Cd(1)−O(181)^{ii}	86.32(8)
Cd(1)−N(31)	2.361(2)	O(181)^{ii}−Cd(1)−O(182)^{ii}	53.23(7)
Cd(1)−N(32)^{i}	2.325(2)	O(182)^{ii}−Cd(1)−O(171)	83.67(7)
Cd(1)−O(181)^{ii}	2.486(2)	N(21)−Cd(1)−N(32c)	164.00(9)
Cd(1)−O(182)^{ii}	2.452(2)	N(21)−Cd(1)−O(172)	92.20(8)
C(17)−O(171)	1.258(4)	N(21)−Cd(1)−N(31)	93.07(9)
C(17)−O(172)	1.259(4)	N(32)^{i}−Cd(1)−O(172)	94.43(8)
C(18)−O(181)	1.280(3)	N(32)^{i}−Cd(1)−N(31)	102.18(9)
C(18)−O(182)	1.246(3)		

[a] Symmetry codes used to generate equivalent atoms: (i) 1/2 − *x*, 1/2 + *y*, 1/2 − *z*; (ii) 1/2 + *x*, 1/2 − *y*, 1/2 + *z*.

Table 3. Selected Bond Lengths (in Å) and Angles (in degrees) for **II**[a]

Cd(1)−O(171)	2.484(9)	O(171)−Cd(1)−O(172)	54.1(3)
Cd(1)−O(172)	2.322(8)	O(172)−Cd(1)−O(192)^{iii}	83.9(3)
Cd(1)−O(11)	2.341(8)	O(192)^{iii}−Cd(1)−O(191)^{iii}	52.2(3)
Cd(1)−N(21)	2.331(11)	O(191)^{iii}−Cd(1)−N(21)	86.2(4)
Cd(1)−O(191)^{iii}	2.333(8)	N(21)−Cd(1)−O(171)	84.1(3)
Cd(1)−O(192)^{iii}	2.574(10)	O(11)−Cd(1)−N(22)^{ii}	167.4(4)
Cd(1)−N(22)^{ii}	2.336(9)	O(11)−Cd(1)−N(21)	94.5(3)
C(17)−O(171)	1.234(14)	O(11)−Cd(1)−O(171)	93.4(3)
C(17)−O(172)	1.261(15)	N(22)^{ii}−Cd(1)−N(21)	98.1(4)
C(19)−O(191)	1.249(16)	N(22)^{ii}−Cd(1)−O(171)	88.5(3)
C(19)−O(192)	1.251(15)		

[a] Symmetry codes used to generate equivalent atoms: (ii) 1/2 + *x*, 1/2 − *y*, 1/2 + *z*; (iii) *x*, −*y*, *z* − 1/2.

metallic centers (in $[Cd_{1.5}(BTC)(BPE)(H_2O)_2]\cdot H_2O$ both Cd^{2+} metal centers were six-coordinated). However, the increased flexibility of the TMD ligands, when compared to those of BPE, leads to less well ordered crystal structures (see below), which should influence the average Cd−O and Cd−N bond lengths. The Cd−O bond length for the coordinated solvent molecule in **II** is 2.341(8) Å, which, just as for $[Cd_{1.5}(BTC)(BPE)(H_2O)_2]\cdot H_2O$,[13] is consistent with reported results.[22]

Unlike in $[Cd_{1.5}(BTC)(BPE)(H_2O)_2]\cdot H_2O$,[13] both metallic structural repeating motifs are surrounded by a large number

(22) Bakalbassis, E. G.; Korabik, M.; Michailides, A.; Mrozinski, J.; Raptopoulou, C.; Skoulika, S.; Terzis, A.; Tsaousis, D. *J. Chem. Soc., Dalton Trans.* **2001**, 850; Yang, G.; Zhu, H. G.; Liang, B. H.; Chen, X. M. *J. Chem. Soc., Dalton Trans.* **2001**, 580; Evans, O. R.; Lin, W. B. *Inorg. Chem.* **2000**, *39*, 2189; Wang, Z. Y.; Xiong, R. G.; Foxman, B. M.; Wilson, S. R.; Lin, W. B. *Inorg. Chem.* **1999**, *38*, 1523.

Table 4. Hydrogen-Bonding Geometry for **I** (in Å and Degrees)[a]

D−H···A	d(D···A)	< (D−H···A)
O(1W)−H(11)···O(2W)	2.794(5)	144(5)
O(1W)−H(12)···O(5W)	2.830(6)	162(6)
O(2W)−H(22)···O(1W)	2.794(5)	171(5)
O(2W)−H(21)···O(8W)	2.812(6)	167(6)
O(3W)−H(32)···O(171)^{i}	2.816(4)	105(5)
O(3W)−H(31)···O(2W)^{ii}	2.755(5)	172(7)
O(4W)−H(42)···O(181)^{i}	2.762(4)	173(6)
O(4W)−H(41)···O(3W)	2.606(5)	95(6)
O(5W)−H(51)···O(7W)	2.755(7)	148(6)
O(5W)−H(52)···O(4W)^{iii}	3.067(8)	132(5)
O(6W)−H(62)···O(182)^{i}	2.792(5)	108(7)
O(7W)−H(71)···O(7W)^{iv}	2.755(9)	146(6)
O(7W)−H(72)···O(8W)^{iv}	2.799(8)	152(7)
O(8W)−H(82)···O(2W)	2.812(6)	117(7)
O(8W)−H(81)···N(22)^{iii}	2.744(6)	150(7)
O(191)−H(191)···O(4W)	2.551(4)	175(4)
O(9W)−H(91)···O(192)^{v}	2.886(8)	158(4)
O(9W)−H(92)···O(192)^{i}	2.752(9)	92(10)

[a] Symmetry codes used to generate equivalent atoms: (i) 1/2 − *x*, −1/2 + *y*, 1/2 − *z*; (ii) −1/2 + *x*, 1/2 − *y*, −1/2 + *z*; (iii) −1/2 + *x*, 1/2 − *y*, 1/2 + *z*; (iv) −*x*, −*y*, 1 − *z*; (iii) 1/2 + *x*, 1/2 − *y*, 1/2 + *z*.

of uncoordinated water molecules (eight and a half and five for **I** and **II**, respectively), which could be the result of the crystallization method used to obtain the single crystals (hydrothermal synthesis followed by Ostwald ripening allowed the inclusion of more water molecules into the structures), and the less well ordered structures due to the increased flexibility of TMD.

In both compounds, the trimesate residues have one uncoordinated and protonated carboxylic acid group [$HBTC^{2-}$; groups C(19) and C(18) for **I** and **II**, respectively], pointing toward the cavities within the structure and strongly hydrogen bonded to uncoordinated water molecules (Figure 6 and Table 4). Consequently, in **I** and **II** $HBTC^{2-}$ acts only as an exo-bidentate bridging ligand forming asymmetric syn,syn-chelates with the Cd^{2+} metal centers, imposing separations of Cd(1)···Cd(1)^{i} 9.9710(2) Å and Cd(1)···Cd(1)^{ii} 9.2947(11) Å for **I** and **II**, respectively [symmetry codes: (i) −1/2 + *x*, −1.5 + *y*, −1/2 + *z*; (ii) *x*, 1 − *y*, −1/2 + *z*;]. As in $[Cd_{1.5}(BTC)(BPE)(H_2O)_2]\cdot H_2O$,[13] the planes of the carboxylate groups are not coplanar with that of the aromatic ring: **I** has the more significant angles [C(17) ca. 26°, C(18) ca. 8°, C(19) ca. 10°], while in **II** two groups lie almost in the plane of the aromatic ring [C(17) ca. 2°, C(18) ca. 1°, C(19) ca. 13°]. It is also interesting to note that the uncoordinated carboxylic acid groups usually have the smallest dihedral angle relative to the plane of the aromatic ring.

In **I**, TMD molecules have two distinct coordination modes: bidentate TMD establishes a physical bridge between Cd^{2+} cations [N(31) and N(32) as donor atoms; Figure 1] imposing a Cd(1)···Cd(1)^{iii} separation of 13.0496(3) Å [symmetry code: (iii) 1/2 − *x*, 1/2 + *y*, 1.5 − *z*]; one TMD ligand is coordinated only to Cd(1) via one 4-pyridyl group [N(21) donor atom; see Figure 1], while the other aromatic group is engaged in a strong O−H···N hydrogen bond with the crystallization O(8W) water molecule (Figure 6 and Table 4). In **II**, all the TMD molecules are coordinated in a bidentate-bridging fashion [N(21) and N(22) as donor atoms; Figure 2], with a Cd(1)···Cd(1)^{iv} separation of 12.2730(13) Å [symmetry code: (iv) 1/2 + *x*, 1/2 − *y*, 1/2 + *z*]. The

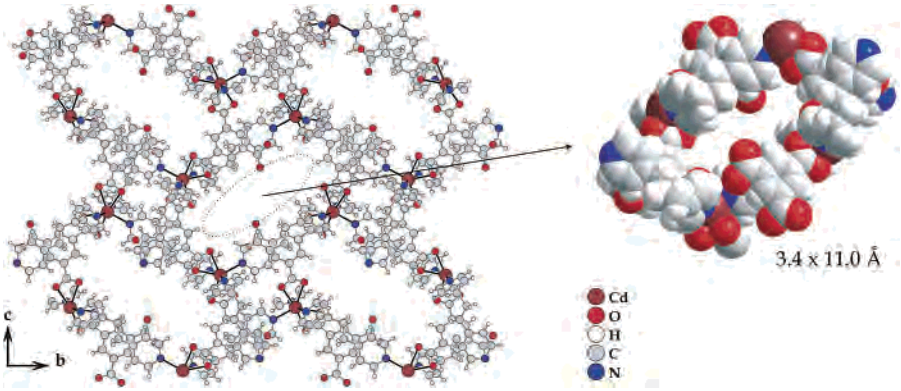

Figure 3. View toward the *bc* plane of the two-dimensional [Cd(HBTC)(TMD)$_2$] framework in **I**. The pores have a cross-section of ca. 3.4 × 11.0 Å based on van der Waals radii (space-filling representation on the right), and are distributed in a distorted herringbone manner.

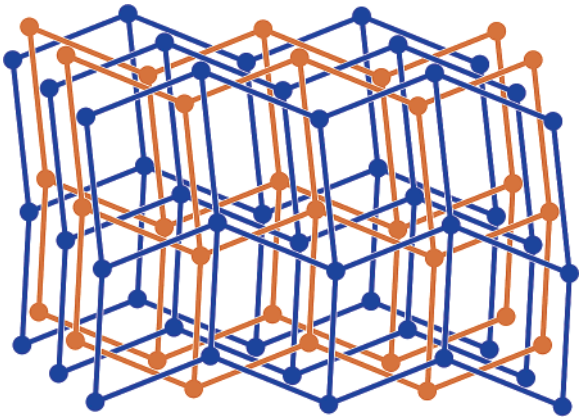

Figure 4. View toward the ($\bar{4}$ 1 8) plane of the topological representation of **I**, showing the four-connected identical plane [Cd(HBTC)(TMD)$_2$] nets packing in an [ABAB···] fashion. Circles (nodes of the framework) are the Cd^{2+} cations. The 4-gons have dimensions of 9.9710(2) and 13.0496(3) Å, which represent the $HBTC^{2-}$ ("short-horizontal" connections) and TMD ("long-vertical" connections) bridging ligands.

high flexibility of the TMD molecules due to the presence of three methylene groups between the 4-pyridyl groups (implying significant dihedral angles between the planes of the rings), along with the different coordination fashions (particularly the unidentate mode) are the direct causes of the different dimensionalities of **I** and **II**.

The repetition of the {CdO_4N_3} metallic structural motif of **I** originates an infinite 2D undulating [Cd(HBTC)(TMD)$_2$] framework placed in the (1 0 $\bar{1}$) plane of the unit cell, with rectangular pores ca. 3.4 × 11.0 Å in cross-section and distributed in a herringbone manner (Figure 3). Considering each Cd^{2+} metal center as a node, the [Cd(HBTC)(TMD)$_2$] framework can be seen as a four-connected plane net with rectangles describing a (4,4) topology (Figure 4).[23] The crystal structure of **I** is obtained by parallel packing of the single 2D framework in an [ABAB···] fashion as shown in Figures 4 and 5. Structural cohesion is achieved by the exo-uncoordinated 4-pyridyl groups of the unidentate TMD between the two adjacent layers occupying the void spaces which act as "clamps" (Figure 5). The crystal structure of **I** contains several channels, also distributed in a herringbone fashion, which are filled by the 8.5 crystallographically

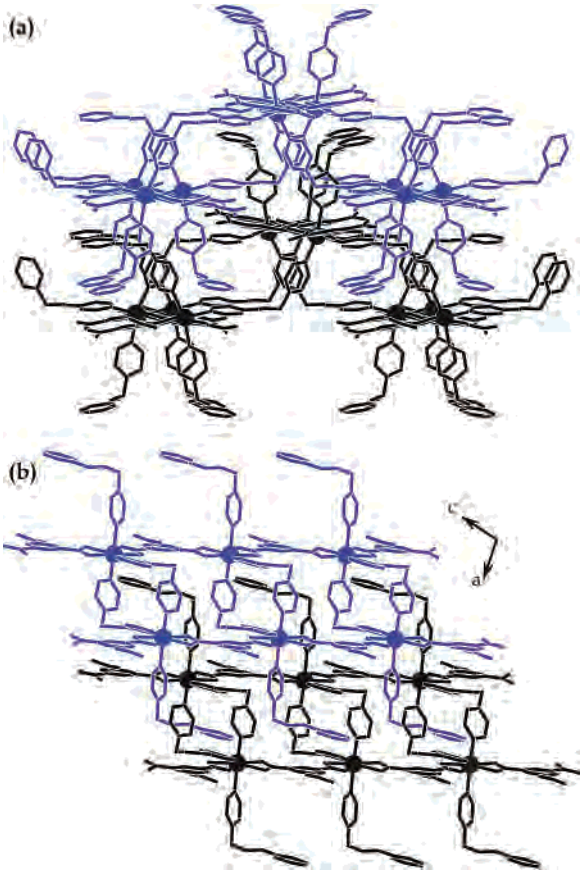

Figure 5. Packing of adjacent [Cd(HBTC)(TMD)$_2$] frameworks (in black- and blue-filled bonds) along the (a) (13 $\bar{1}$ 16) plane and the (b) *b* crystallographic direction, showing the unidentate TMD ligands acting as "clamps" by occupying the void spaces of the neighboring frameworks. Hydrogen atoms have been omitted for clarity.

unique uncoordinated water molecules involved in strong O−H···O and O−H···N hydrogen bonds (Figure 6 and Table 4). Such interactions establish physical connections between neighboring undulated [Cd(HBTC)(TMD)$_2$] layers.

Compound **II** has a porous 3D framework, [Cd(HBTC)−(TMD)(H_2O)], with channels running in several directions. The most prominent cavities are ca. 3.2 × 13.2 Å in cross-section and run along the *c* axis (Figure 7, top). It seems that the brick-wall distribution of these channels is a direct consequence of the high flexibility of TMD, in which the two 4-pyridyl groups lie in planes almost perpendicular to

(23) Wells, A. F. *Structural Inorganic Chemistry*; 4th ed.; Clarendon Oxford University Press: New York, 1975.

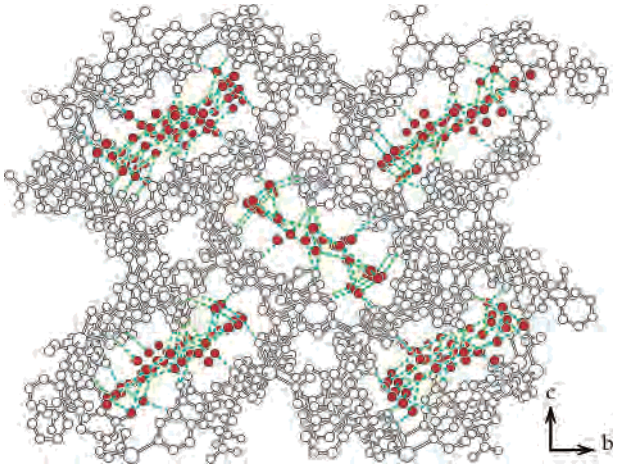

Figure 6. Crystal packing of **I** showing the uncoordinated crystallization water molecules lying inside the one-dimensional channels (see Figure 3) and strongly hydrogen-bonded to the neighboring [Cd(HBTC)(TMD)$_2$] layers (represented with white-filled bonds and atoms). Hydrogen atoms have been omitted for clarity, and hydrogen bonds are represented as green-filled dashed bonds. For hydrogen-bonding geometry see Table 4.

each other (Figure 7, top). Furthermore, as in structure [$Cd_{1.5}$(BTC)(BPE)(H_2O)$_2$]·H_2O,[13] the coordinated water molecules are oriented toward the interior of the channels, which may facilitate their removal. Other rectangular-shaped, but smaller, channels with cross-section of ca. 6.0 × 3.0 Å are parallel to the *a* direction and distributed in a herringbone manner (see Figure 7).

Adopting the node assignment used for structure **I** (i.e., each Cd^{2+} is considered as a node), the [Cd(HBTC)(TMD)(H_2O)] framework in **II** can be, according to Wells, classified as a typical diamondoid (6,4) net (Figure 8a).[23] However, as previously mentioned, this is not a regular diamondoid net because of the presence of two distinct intermetallic distances [the $HBTC^{2-}$ bridge imposes a Cd(1)···Cd(1)^{ii} separation of 9.2947(11) Å, while for the TMD bridge Cd(1)···Cd(1)^{iv} is of 12.2730(13) Å; symmetry codes: (ii) x, $1 - y$, $-1/2 + z$; (iv) $1/2 + x$, $1/2 - y$, $1/2 + z$].

As in [$Cd_{1.5}$(BTC)(BPE)(H_2O)$_2$]·H_2O,[13] the channels of [Cd(HBTC)(TMD)(H_2O)] are filled by another identical framework in a typical 2-fold interpenetration fashion (Figure 8). However, as seen in Figure 8b, the two interpenetrated frameworks are not displaced (along the *a* axis) of the usual one-half of the length of the adamantane unit. The reason is again the high conformational flexibility of the bridging TMD ligand, with the three methylene groups avoiding closer proximity of the two [Cd(HBTC)(TMD)(H_2O)] frameworks (Figure 8b).

The four-and-a-half crystallographically unique uncoordinated crystallization water molecules are inside the crystal cavities left empty after the interpenetration of the two identical [Cd(HBTC)(TMD)(H_2O)] nets (see Supporting Information, Figure S2; Table 5). These molecules are strongly hydrogen bonded and, as in the previously described compound, establish links between neighboring frameworks (see Supporting Information, Figure S3; Table 5). Thus, cooperative O−H···O interactions connect carboxylate groups and uncoordinated crystallization water molecules [O(1W) and O(4W)], forming hydrogen-bonded chains between the two interpenetrating frameworks. Furthermore, the coordinated water molecule O(11) from one framework is O−H···O hydrogen-bonded to the C(17) carboxylate group [O(172) atom] from the other framework, leading to the formation of a typical $R_2^2(8)$ graph set motif.

Crystal Structure of [Cd_2(BTC)(TMD)$_2$(NO_3)]·3H_2O (III). While compounds **I** and **II** could only be obtained in significant amounts after Ostwald ripening of the autoclave contents, large crystals of another Cd−OF, also containing TMD ligands, could be directly obtained from the autoclave product by simply changing the experimental conditions: following our systematic study of the synthesis of [Cd(NDC)(H_2O)] (where NDC^{2-} = 2,6-naphthalenedicarboxylate),[20] the content of metal cations in the reactive mixture was significantly increased, and the autoclaves were left at a higher temperature of 145 °C for a longer period of time (see Experimental Section). Single crystals suitable for X-ray diffraction were manually selected and formulated as [Cd_2(BTC)(TMD)$_2$(NO_3)]·3H_2O (**III**).

The structure contains two crystallographically unique Cd^{2+} metal centers, with hepta- and hexacoordinated distorted pentagonal bipyramidal and octahedral coordination fashions for Cd(1) and Cd(2), respectively (Figure 9 and Tables 6 and 7). As in **I** and **II**, the classification of the coordination environment for Cd(1) as a distorted pentagonal bipyramid is again caused by the difference in the Cd−O bond lengths for the coordinated C(17) and C(19) carboxylate groups (Figure 9 and Table 6). However, in **III** the bond length difference is smaller [in particular, for the C(19) carboxylate group; see Table 6]. Cd(1) is coordinated to two BTC^{3-} and three TMD ligands, {CdO_4N_3} (Figure 9a and Table 6), while Cd(2) has in its coordination sphere three BTC^{3-}, one TMD ligand and one nitrate anion (NO_3^-), {CdO_5N} (Figure 9b and Table 6). The average Cd−O and Cd−N bond lengths are 2.39 and 2.33 Å, respectively, in very good agreement with the values for **I** and **II**, also reflecting the increase in the coordination number [of Cd(1)] when compared to those in structure [$Cd_{1.5}$(BTC)(BPE)(H_2O)$_2$]·H_2O.[13]

An interesting feature in **III** is the presence of a coordinated nitrate ion within the coordination sphere of Cd(2) (Figure 9b). Such a structural motif has been found in several other MOFs containing either H_3BTC,[12] BPE,[24] or TMD.[15] In the case of the compact structure **III**, the nitrate ions (present in the reactive mixture as the counterions in the metallic salt) have the ideal size to occupy the small available spaces, thus compensating the charge of the hypothetical [Cd_2(BTC)(TMD)$_2$]$^+$ framework and allowing their coordination to the Cd^{2+} centers.

As for structure [$Cd_{1.5}$(BTC)(BPE)(H_2O)$_2$]·H_2O,[13] BTC^{3-} appears as an exo-tridentate bridging ligand forming two coordinative η^3-syn,syn-bimetallic-bridging-chelates, C(17) and C(19), and one η^3-syn,syn-chelate bond, C(18) (Figure

(24) Hennigar, T. L.; MacQuarrie, D. C.; Losier, P.; Rogers, R. D.; Zaworotko, M. J. *Angew. Chem., Int. Ed.* **1997**, *36*, 972; Sharma, C. V. K.; Rogers, R. D. *Chem. Commun.* **1999**, 83; Power, K. N.; Hennigar, T. L.; Zaworotko, M. J. *Chem. Commun.* **1998**, 595; Fujita, M.; Kwon, Y. J.; Miyazawa, M.; Ogura, K. *Chem. Commun.* **1994**, 1977; Fujita, M.; Aoyagi, M.; Ogura, K. *Bull. Chem. Soc. Jpn.* **1998**, *71*, 1799.

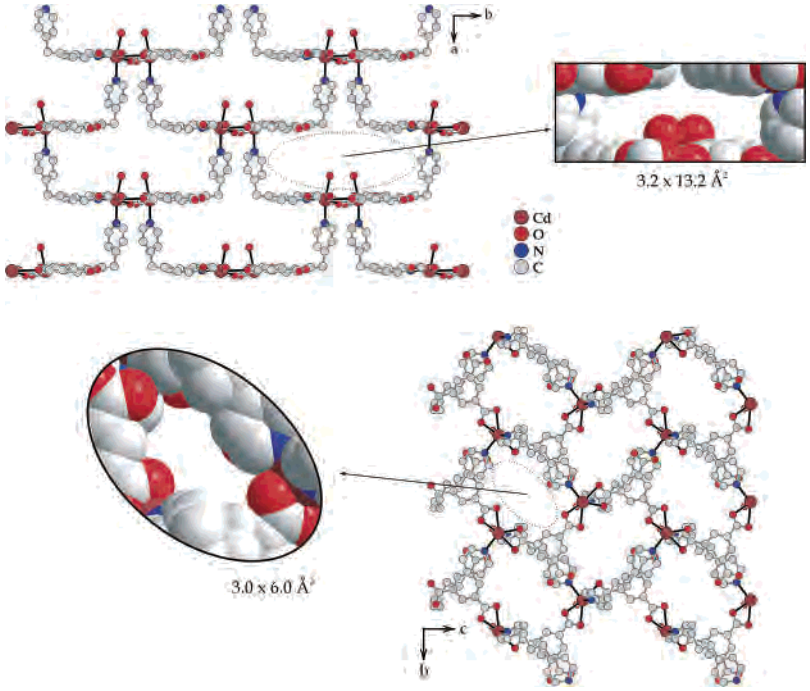

Figure 7. Projections along the *c* (top) and *a* (bottom) directions of the three-dimensional [Cd(HBTC)(TMD)(H_2O)] framework in **II** showing the different types of cavities. Hydrogen atoms have been omitted for clarity, and cross-sections have been calculated based on van der Waals radii (space-filling representations).

10a). The ligand establishes connections between five neighboring Cd^{2+} metal centers (for intermetallic distances and symmetry codes see the caption to Figure 10), leading to the formation of an almost planar one-dimensional zigzag [Cd_2(BTC)(NO_3)] tape running along the *a* direction. Cd(2) metal centers are alternately above and below the plane of the BTC^{3-} and Cd(1) ions (Figure 10b,c).

The close proximity of BTC^{3-} ligands within the [Cd_2(BTC)(NO_3)] tape suggests that they could be linked via weak C−H···O interactions, as described in the organic crystal [($BPEH_2$)(H_2BTC)$_2$(H_3BTC)$_2$·H_2O].[16] While this could be true for C(12)−H(12A)−O(181) [3.538(13) Å; symmetry code: (ii) $-x$, $1-y$, $1-z$] with an angle for the interaction very close to the linearity (167.4°), for C(14)···H(14A)···O(182) [3.388(13) Å; symmetry code: (ii) $-1-x$, $1-y$, $1-z$], the angle is only 132.8°, which makes such interaction unlikely.

Although the three carboxylate groups of BTC^{3-} have equivalent C−O bonds (in the 1.24−1.28 Å range), the Cd−O bonds are in the 2.23−2.54 Å range (Figure 9 and Table 6). This can be explained by the large Cd^{2+}/ligands ratio (1:2), which creates a strained framework to accommodate all the Cd^{2+} cations, and thus leads to distorted coordination fashions for the carboxylate groups. This assumption is supported by the fact that none of the carboxylate groups are coplanar with the benzene aromatic ring [average dihedral angles of ca. 13°, 23°, and 19° for C(17), C(18), and C(19), respectively], as in the previous structures.

As in **II**, TMD molecules appear in **III** as bidentate-bridging ligands connecting neighboring [Cd_2(BTC)(NO_3)] tapes (Figures 10 and 12) and imposing Cd(1)···Cd(1)^{i} and Cd(1)···Cd(2)^{ii} separations of 12.7251(12) and 13.6541(10) Å, respectively [symmetry codes: (iii) $1/2-x$, $1/2+y$, $1/2-z$; (iv) $-1/2+x$, $1/2-y$, $1/2+z$]. The increased flexibility of this molecule is again one of the main causes for the crystal structure of **III**: on one hand, and similarly to that found for **II**, the presence of only bidentate-bridging TMD ligands leads to a 3D structure; on the other hand, the flexibility of the three methylene groups along with the high metal content leads to a compact structure (with no interpenetration, see below).

The two crystallographically unique Cd^{2+} metal centers are bridged by the C(17) and C(19) carboxylate groups, forming a binuclear secondary building unit (SBU), [Cd_2(BTC)$_4$(NO_3)(TMD)$_4$], in which the intermetallic Cd(1)···Cd(2) separation is 3.6435(10) Å (Figure 11). The 3D assembly of this binuclear SBU leads to a compact (i.e., nonporous), neutral, and coordinatively bonded framework, [Cd_2(BTC)(TMD)$_2$(NO_3)] (Figure 12). Taking the geometrical centers of the SBU as nodes for this framework, the structure of **III** can be described as an irregular eight-connected net in which the smallest circuits comprise three and four nodes, with the complete topological representation being an unusual $3^6 4^{22}$ (Figure 13).[23]

The three crystallographically unique crystallization water molecules occupy the small available spaces and are strongly hydrogen bonded (via O−H···O and O−H···O− interactions) to the neutral [Cd_2(BTC)(TMD)$_2$(NO_3)] framework (Figures 12 and S4 in Supporting Information; Table 8).

Thermal Analysis. Thermal decomposition of the mixture of **I** with **II** does not occur with well-defined weight losses. The major weight losses only occur above ca. 300 °C, probably as a result of oxidation to CdO, thus showing some thermal stability up to this temperature, releasing only the crystallization solvent below this temperature.

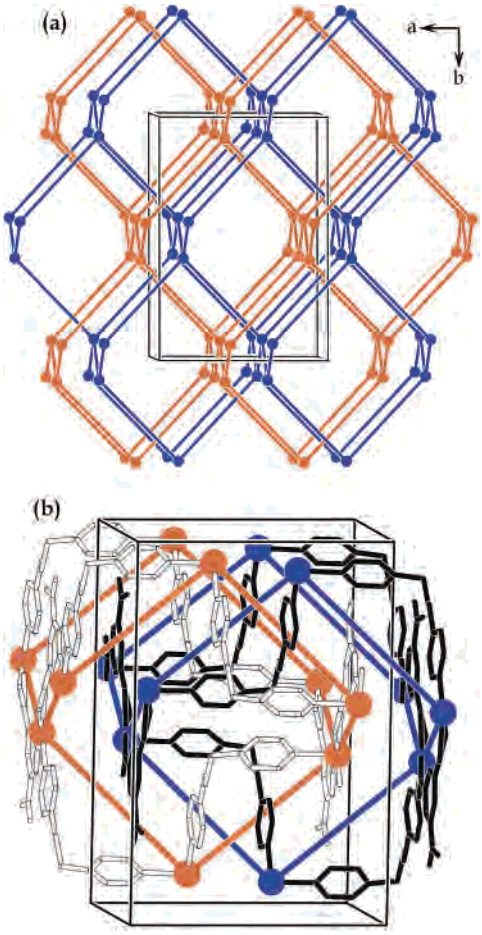

Figure 8. (a) Topological representation of structure **II** showing the 2-fold interpenetration of irregular (6,4) diamond nets: the Cd^{2+} cations are taken as nodes of the [Cd(HBTC)(TMD)(H_2O)] framework; "long" connections between metal centers correspond to TMD bridges [12.2730(13) Å], while "short" connections represent the $HBTC^{2-}$ bridges [9.2947(11) Å]. In (b) topological connections are overlapped with the crystal packing (the two frameworks are represented with white- and black-filled bonds; hydrogen atoms and crystallization water molecules were also omitted for clarity).

Table 5. O···O Short Contacts for **II** (in Å)[a]

D···A	d(D···A)
O(11)···O(172)^{i}	2.835(5)
O(11)···O(1W)	2.770(5)
O(181)···O(3W)^{ii}	2.750(5)
O(1W)···O(4W)	2.953(6)
O(2W)···O(181)^{iii}	3.061(5)
O(3W)···O(191)^{iii}	2.833(6)
O(3W)···O(181)^{ii}	2.750(5)
O(4W)···O(171)	2.775(5)
O(4W)···O(182)^{iv}	2.974(5)
O(5W)···O(3W)^{ii}	2.787(7)

[a] Symmetry codes used to generate equivalent atoms: (i) $-x, 1-y, -z$; (ii) $-x, -y, -z$; (iii) $-1/2+x, 1/2-y, -1/2+z$; (iv) $-x, y, 1/2-z$.

As expected from its structure (see single-crystal refinement details), compound **III** loses more water molecules per formula unit than the three molecules in the empirical formula. In a slow multistep process, a total weight loss of 10.0% between ambient temperature and 205 °C is in very good agreement with the calculated value for six water molecules (10.8%). However, in view of the limitations described in the single-crystal analysis section, the extra

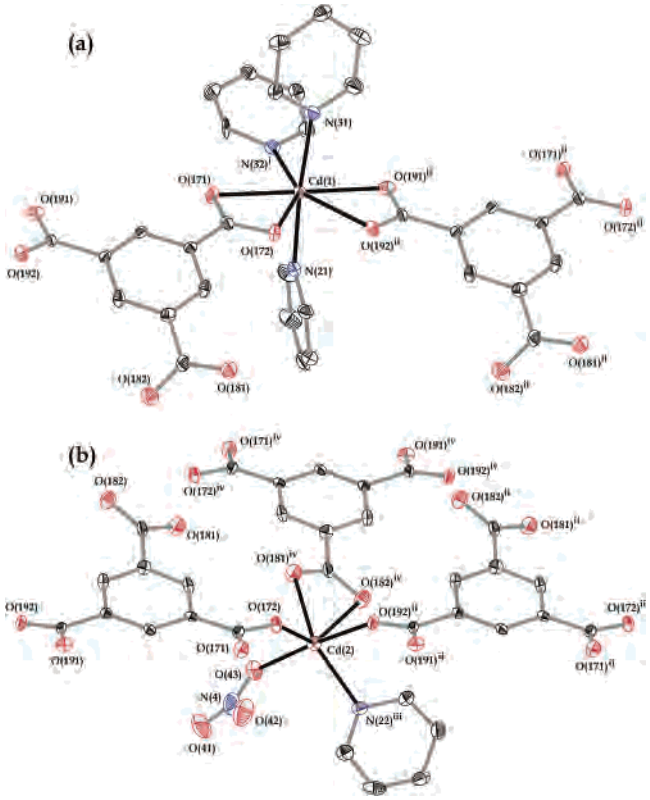

Figure 9. (a, b) Schematic representation of the distorted octahedral coordination environments for the two crystallographically unique Cd^{2+} metal centers in **III**. Thermal ellipsoids are drawn at the 30% probability level. For clarity, TMD ligands are represented by only one 4-pyridyl group, and hydrogen atoms have been omitted. For bond lengths (in Å) and angles (in degrees) see Tables 6 and 7, respectively. Symmetry codes used to generate equivalent atoms: (i) $1/2-x, -1/2+y, 1/2-z$; (ii) $x+1, y, z$; (iii) $x+1/2, 1/2-y, -1/2+z$; (iv) $-x, 1-y, 1-z$.

Table 6. Selected Bond Lengths (in Å) for **III**[a]

Cd(1)−N(21)	2.322(8)	Cd(1)−O(192)^{ii}	2.454(7)
Cd(1)−N(31)	2.354(8)	Cd(2)−N(22)^{iii}	2.273(8)
Cd(1)−N(32)^{i}	2.311(8)	Cd(2)−O(172)	2.234(7)
Cd(1)−O(171)	2.499(7)	Cd(2)−O(181)^{iv}	2.272(8)
Cd(1)−O(172)	2.375(7)	Cd(2)−O(182)^{iv}	2.542(8)
Cd(1)−O(191)^{ii}	2.423(7)	Cd(2)−O(192)^{ii}	2.353(7)
		Cd(2)−O(43)	2.366(10)
C(17)−O(171)	1.248(12)	C(18)−O(182)	1.256(13)
C(17)−O(172)	1.281(11)	C(19)−O(191)	1.274(12)
C(18)−O(181)	1.268(13)	C(19)−O(192)	1.267(11)

[a] Symmetry codes used to generate equivalent atoms: (i) $1/2-x, -1/2+y, 1/2-z$; (ii) $x+1, y, z$; (iii) $x+1/2, 1/2-y, -1/2+z$; (iv) $-x, 1-y, 1-z$.

solvent could not be satisfactorily included in the crystal solution. Thermal decomposition of **III** proceeds with two weight losses of 13.7 and 36.5% in the 255−320 and 320−560 °C temperature ranges, respectively, which, as for the previous compounds, is also attributed to a multistep oxidation of the organic component (shoulders in the DTG peaks, along with several and very close processes indicated by DSC measurements). In this case, the measured residue after "total" decomposition does not agree with the formation of the stoichiometric amount of CdO (calculated: 25.7%; observed: 39.8%). The gradual and very slow weight loss after 600 °C suggests that the residue still contains an organic component. This is confirmed by elemental analysis, explaining the high value obtained for the TGA residue.

Table 7. Selected Bond Angles (in degrees) for **III**[a]

N(21)−Cd(1)−N(31)	174.7(3)	N(22)^{iii}−Cd(2)−O(43)	90.3(3)
N(21)−Cd(1)−O(171)	95.4(3)	N(22)^{iii}−Cd(2)−O(182)^{iv}	86.6(3)
N(21)−Cd(1)−O(172)	88.9(3)	N(22)^{iii}−Cd(2)−O(192)^{ii}	87.2(3)
N(21)−Cd(1)−O(191)^{ii}	87.2(3)	O(43)−Cd(2)−O(182)^{iv}	95.9(3)
N(21)−Cd(1)−O(192)^{ii}	85.5(3)	O(172)−Cd(2)−O(43)	105.4(3)
N(31)−Cd(1)−O(171)	89.9(3)	O(172)−Cd(2)−O(181)^{iv}	91.8(3)
N(31)−Cd(1)−O(172)	94.5(3)	O(172)−Cd(2)−O(182)^{iv}	136.4(3)
N(31)−Cd(1)−O(191)^{ii}	87.5(3)	O(172)−Cd(2)−O(192)^{ii}	73.2(2)
N(31)−Cd(1)−O(192)^{ii}	91.9(3)	O(172)−Cd(2)−N(22)^{iii}	129.9(3)
N(32)^{i}−Cd(1)−N(21)	92.9(3)	O(181)^{iv}−Cd(2)−O(43)	80.3(3)
N(32)^{i}−Cd(1)−N(31)	86.6(3)	O(181)^{iv}−Cd(2)−N(22)^{iii}	138.1(3)
N(32)^{i}−Cd(1)−O(171)	92.1(3)	O(181)^{iv}−Cd(2)−O(192)^{ii}	104.4(3)
N(32)^{i}−Cd(1)−O(172)	145.6(3)	O(192)^{ii}−Cd(2)−O(43)	175.1(3)
N(32)^{i}−Cd(1)−O(191)^{ii}	91.6(3)	O(192)^{ii}−Cd(2)−O(182)^{iv}	88.2(2)
N(32)^{i}−Cd(1)−O(192)^{ii}	145.4(3)		
O(172)−Cd(1)−O(191)^{ii}	122.8(2)		
O(172)−Cd(1)−O(192)^{ii}	69.0(2)		
O(191)^{ii}−Cd(1)−O(171)	175.3(2)		
O(192)^{ii}−Cd(1)−O(171)	122.4(2)		
Cd(1)−O(191)^{ii}	2.423(7)		

[a] Symmetry codes used to generate equivalent atoms: (i) $1/2 - x, -1/2 + y, 1/2-z$; (ii) $x + 1, y, z$; (iii) $x + 1/2, 1/2 - y, -1/2 + z$; (iv) $-x, 1 - y, 1 - z$.

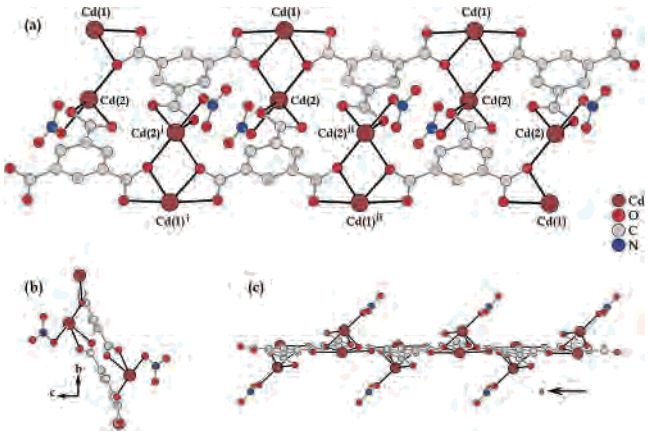

Figure 10. Zigzag one-dimensional $[Cd_2(BTC)(NO_3)]$ tape, present in the structure of **III**, which runs along the *a* direction. Cd(1)···Cd(2) 3.6435(10) Å. Cd(2)···Cd(2)^{i} 7.2436(15) Å. Cd(2)···Cd(2)^{ii} 8.1882(15) Å. Cd(2)···Cd(1)^{i} 9.3231(11) Å. Cd(2)···Cd(1)^{ii} 9.9365(11) Å. Hydrogen atoms have been omitted for clarity. Symmetry codes used to generate equivalent atoms: (i) $-x, 1 - y, 1 - z$; (ii) $1 - x, 1 - y, 1 - z$.

Vibrational Spectroscopy. The typical vibrations of substituted benzene and/or pyridine aromatic rings, and the vibrational modes for carboxylic acid groups in the IR and Raman spectra, confirm the presence of H_3BTC and TMD in compounds **I** to **III**. The extensive hydrogen-bonding network present within the crystal structures, which involves the coordinated and uncoordinated solvent molecules, is also markedly observed in the spectra through the ν(O−H), δ(O−H···O), and γ(O−H···O) vibrational modes.

The Δ values, defined by Deacon and Phillips as $\nu_{asym}(\text{-}CO_2^-) - \nu_{sym}(\text{-}CO_2^-)$,[25] give some qualitative structural information concerning the coordination modes of the carboxylate groups and are summarized in Table 9. While the smaller values of Δ are consistent with the chelating coordinative fashion, the larger values could indicate the existence of unidentate coordinated carboxylate groups (Table 9). As described by single-crystal analysis, such a

(25) Deacon, G. B.; Phillips, R. J. *Coord. Chem. Rev.* **1980**, *33*, 227.

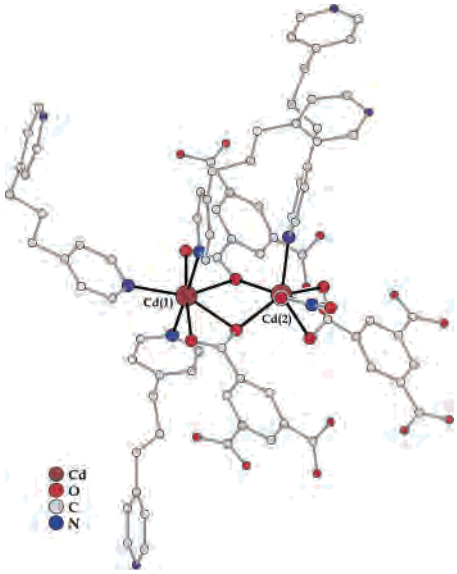

Figure 11. Binuclear secondary building unit (SBU) present in **III**. The distance between the two Cd^{2+} metal centers Cd(1)···Cd(2) is 3.6435(10) Å. Hydrogen atoms have been omitted for clarity.

coordination mode does not appear in any of the structures. Deacon and Phillips suggest a possible explanation for these large values for Δ: considering the existence of a highly asymmetric chelate within the structures, the coordination modes could be seen as approaching the unidentate form. As mentioned, structures **II** and **III** contain carboxylate groups [C(19) and C(18), respectively] forming asymmetric chelates with the Cd^{2+} metallic centers (for compound **II** see Figure 2 and Table 3; for compound **III** see Figure 9 and Table 6). Another possible explanation, briefly mentioned by the same authors, is based on the idea that the pressure used to make the KBr pellets (from which the IR spectra were collected; see Experimental Section) might induce a degree of modification in the structures, converting chelating coordination modes to unidentate modes, or at least to asymmetric chelates. This idea should not be disregarded, since the presence of highly flexible TMD organic molecules within the easily distorted multidimensional frameworks of compounds **I**, **II**, and **III** might facilitate such distortions.

Conclusions

Three multidimensional MOFs containing 1,3,5-benzenetricarboxylate anions (H_XBTC^{x-3}) and 4,4′-trimethylenedipyridine (TMD) coordinated to Cd^{2+} metal centers have been prepared and isolated in their crystalline forms. The increased flexibility of TMD was shown to have direct consequences in the type and properties of the products. First, while only one compound with H_XBTC^{x-3} anions was always obtained with BPE ($[Cd_{1.5}(BTC)(BPE)(H_2O)_2]\cdot H_2O$),[13] the use of TMD leads in this case to three different structures (**I**−**III**), sometimes even as a mixture (**I** and **II**). Second, the crystallinity of the products containing TMD was significantly lower. For compounds **I** and **II**, crystals suitable for X-ray analysis could only be obtained after Ostwald ripening. TMD thus seems to lead to less ordered crystal structures, which tend to crystallize preferentially as microcrystalline

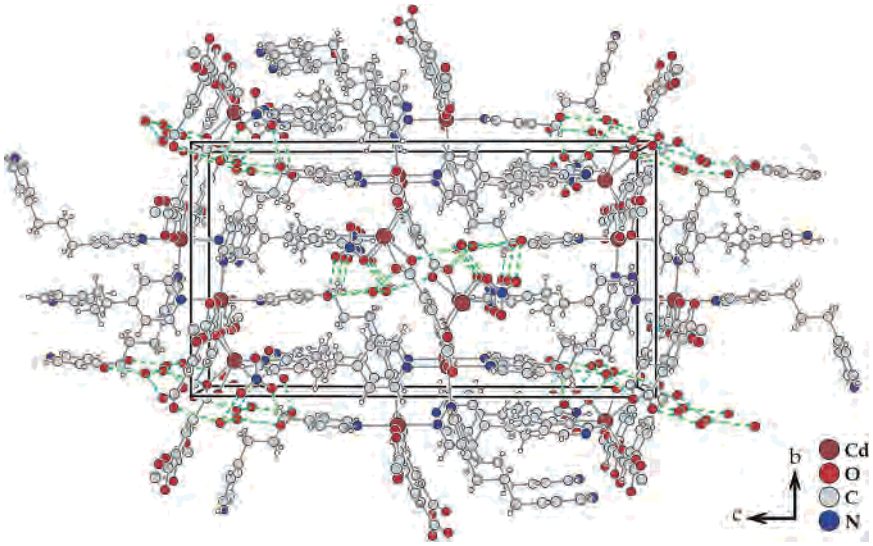

Figure 12. Crystal packing of **III** showing the hydrogen bonds (green dashed lines) between the crystallization water molecules and three-dimensional $[Cd_2(BTC)(TMD)_2(NO_3)]$ framework. For O···O contacts see Table 8.

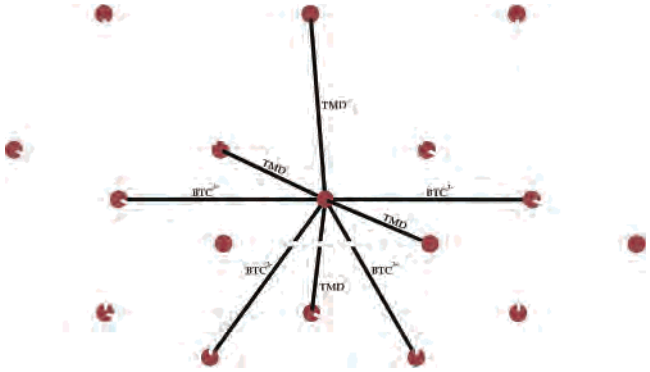

Figure 13. Topological representation of a portion of the $[Cd_2(BTC)(TMD)_2(NO_3)]$ framework showing the environment around an eight-connected node. TMD and BTC^{3-} bridges between connected nodes are indicated.

Table 8. O···O Short Contacts for III (in Å)[a]

D···A	d(D···A)
O(1W)···O(181)^{i}	2.764(13)
O(1W)···O(43)^{i}	2.871(14)
O(2W)···O(1W)	2.856(16)
O(2W)···O(3W)	2.872(19)
O(3W)···O(2W)	2.872(19)
O(3W)···O(41)^{i}	2.919(19)

[a] Symmetry code used to generate equivalent atoms: (i) $-x, 1-y, 1-z$.

Table 9. Values of Δ [$\nu_{asym}(-CO_2-) - \nu_{sym}(-CO_2^-)$] for Compounds **I** to **III** (in cm^{-1})[25]

	$\nu_{asym}(-CO_2-)$	$\nu_{sym}(-CO_2^-)$	D
I + II	1559	1436	123
	1613	1369	244
III	1563	1436	127
	1614	1370	244

powders. Work is under way to determine the composition regions where each of the described compounds can be isolated.

Experimental Section

Synthesis. Reagents were obtained from commercial sources and used as received without further purification. Synthesis was carried out in a PTFE-lined stainless steel reaction vessel (8 or 21 cm^3, 70% filling rate), under autogenous pressure and static conditions. Compounds proved to be air- and light-stable, and insoluble in water and in organic solvents such as methanol, ethanol, acetone, dichloromethane, toluene, DMSO, and chloroform.

$[Cd(HBTC)(TMD)_2]\cdot 8.5(H_2O)$ (I) and $[Cd(HBTC)(TMD)(H_2O)]\cdot 4.5(H_2O)$ (II). $Cd(NO_3)_2\cdot 4H_2O$ (0.807 g, Aldrich) was dissolved in distilled water (ca. 7.5 cm^3) at ambient temperature, followed by the addition, with vigorous magnetic stirring, of 4,4′-trimethylenedipyridine (TMD, 0.519 g, Aldrich). A solution of 1,3,5-benzenetricarboxylic acid (H_3BTC, 0.633 g, Aldrich) and triethylamine (TEA, 0.763 g, Avocado) in distilled water (ca. 9 cm^3) was added dropwise to the resulting white suspension. The final mixture, with a molar composition of 1.00 Cd^{2+}/1.00 TMD/1.15 H_3BTC/2.88 TEA/350 H_2O, was stirred thoroughly for 1 h at ambient temperature before being transferred to the reaction vessel, which was sealed and placed inside a preheated oven at 145 °C. The temperature profile used for the synthesis has been reported.[13,19,20] Immediately after opening, the reaction vessel was left undisturbed for 10 weeks in the dark at ambient temperature before single crystals suitable for X-ray diffraction could be manually selected. The powder was then washed with ca. 50 cm^3 of distilled water and ca. 3 × 50 cm^3 of absolute ethanol, and then air-dried at 70 °C.

Elemental composition found for the mixture of **I** with **II**: C 45.03%, H 3.96%, and N 5.58%. TGA data (weight losses) and derivative thermogravimetric peaks (DTG; in italics inside the parenthesis): 40−160 °C 7.0% (*73* and *120* °*C*); 180−305 °C 12.2% (*250* °*C*); 305−450 °C 54.7% (*368*, *387*, and *416* °*C*). DSC peaks: 245, 362, and 400 °C. Selected vibrational (FT-IR and FT-Raman in italics; cm^{-1}): ν(O−H, lattice and coordinated water), 3398vs,vb; ν(C−H, aromatic compounds), 3085m (*3069*); ν_{asym}(C−H in $-CH_2-$), 2985m and 2944m (*2992* and *2049*); ν_{sym}(C−H in $-CH_2$), 2908m and 2863m (*2901* and *2860*); overtones and combination bands for 1,3,5-trisubstituted benzene rings, 1948w, 1875w, and 1710m; $\nu_{asym}(-CO_2^-)$, 1613vs and 1559vs; interactions between ν(C−C) and ν(C−N) for 4-monosubstituted pyridines, 1570m (*1546* and *1570*); ν(-C−H, aromatic compounds), 1535m; from aromatic compounds with groups capable of donating electrons (e.g., carboxylate groups), 1504m (*1502*); $\delta(-CH_2-)$, 1419m (*1418*); ν(C−H, aromatic compounds), (*1451*); $\nu_{sym}(-CO_2^-)$, 1436vs and 1369vs; δ(O−H···O), 1330m (*1330*, *1348*, and *1368*); ν(C−O), 1226m

(*1212*); ρ(C−H), 1187m (*1190*); δ(-C−H, 4-monosubstituted pyridines), 1100m and 1068m (*1073*); δ(═C−H, aromatic compounds), 1018m (*1020* and *1004*); γ(O−H···O), 935m (*938*); δ(C−O), (*834*); γ(═C−H, 4-monosubstituted pyridines), 810m and 797m (*807* and *795*); ω(C−H, substituted benzene rings), 759m (*756*); γ(C−O), 740s (*740*); depolarized δ(C═C) band for substituted aromatic rings, (*668*); ρ[(C−O)−O], 490m and 517m; γ(C−H, aromatic rings), 388m.

$[Cd_2(BTC)(TMD)_2(NO_3)]\cdot 3H_2O$ (III). Compound **III** was prepared by a similar experimental procedure to that for **I** and **II**, but using instead 1.580 g of $Cd(NO_3)_2\cdot 4H_2O$, 0.217 g of H_3BTC, 0.209 g of TMD, 0.328 g of TEA, and ca. 9 g of distilled water. The reactive mixture, with a molar composition of 4.96 Cd^{2+}/1.02 TMD/1.00 H_3BTC/3.14 TEA/486 H_2O, was transferred to a reaction vessel that was placed inside an oven at ambient temperature. The temperature was then increased to 145 °C and maintained unchanged for 8 h. After this time, the temperature was slowly lowered to ambient temperature over 14 h before the reaction vessel was opened. A white microcrystalline product was obtained, from which small single crystals were manually separated under the microscope and preserved in a portion of the autoclave mother liquor. The remaining microcrystalline powder was washed with ca. 50 cm^3 of distilled water and ca. 3 × 50 cm^3 absolute ethanol, and then air-dried at 70 °C.

Elemental composition found: C 45.35%, H 4.11%, and N 8.01%; calculated (based on single-crystal data): C 44.23%, H 4.56%, and N 7.37%. TGA data (weight losses) and derivative thermogravimetric peaks (DTG; in italics inside the parenthesis): 25−205 °C 10.0% (*73 °C*); 255−320 °C 13.7% (*303 °C*); 320−560 °C 36.5% (*393*, *408* and *422 °C*). DSC peaks: 93, 115, 300, 312, 343, 407, 423, and 433 °C. Selected vibrational (FT-IR and FT-Raman in italics; cm^{-1}): ν(O−H, lattice and coordinated water), 3448vs,vb; ν(C−H, aromatic compounds), 3080s (*3080* and *3067*); ν_{asym}(C−H in -CH_2-), 2942m and 2915m (*2942* and *2917*); ν_{sym}(C−H in -CH_2-), 2873m and 2852m (*2875* and *2854*); overtones and combination bands for 1,3,5-trisubstituted benzene rings, 1951w and 1872w; ν_{asym}(-CO_2^-), 1614vs and 1563vs; interactions between ν(C−C) and ν(C−N) for 4-monosubstituted pyridines, 1575m (*1564*); ν(-C−H, aromatic compounds), 1539m; from aromatic compounds with groups capable of donating electrons (e.g., carboxylate groups), 1504w (*1503*); ν(C−H, aromatic compounds), (*1456* and *1442*); ν_{sym}(-CO_2^-), 1436vs and 1370vs; δ(O−H···O), 1332w,sh (*1328*, *1347*, and *1365*); ν(C−O), 1225m and 1229m (*1214*); ρ(C−H), 1188m (*1193*); δ(-C−H, 4-monosubstituted pyridines), 1106m and 1067m (*1069*); δ(═C−H, aromatic compounds), 1017s (*1020* and *1003*); γ(O−H···O), 932m (*938*); δ(C−O), 832m (*832*); γ(═C−H, 4-monosubstituted pyridines), 807m and 797m (*808* and *797*); ω(C−H, substituted benzene rings), 765s; γ(C−O), 737s and 723s (*738*); depolarized δ(C═C) band for substituted aromatic rings, (*668*); γ(C−H, 1,3,5-trisubstituted-benzene rings), (*546*).

Physical Measurements. Elemental analysis for carbon, hydrogen, and nitrogen was performed on an Exeter Analytical CE-440 Elemental analyzer. Samples were combusted under an oxygen atmosphere at 975 °C for 1 min, with helium used as purge gas.

FT-IR spectra were collected from KBr pellets (Aldrich 99%+, FT-IR grade) using a Mattson 4000 at the University of Aveiro, Portugal. FT-Raman spectra were measured on a Bruker RFS 100 with a Nd:YAG coherent laser (λ = 1064 nm) at the University of Aveiro.

Scanning electron microscopy images were obtained in Aveiro using a FEG-SEM Hitachi S4100 microscope operating at 25 kV. Samples were prepared by deposition on aluminum sample holders and by carbon coating.

Thermogravimetric analysis was carried out using a Polymer Laboratories TGA 1500 at the University of Cambridge. Differential scanning calorimetry analysis was performed at the University of Aveiro, using a Shimadzu DSC-50. These thermoanalytical studies were always performed using a heating rate of 5 °C/min and a constant nitrogen flow (rate of 25 cm^3/min).

Single-Crystal X-ray Crystallography. Suitable single crystals were mounted on a glass fiber using perfluoropolyether oil.[26] Data were collected at 180(2) K on a Nonius Kappa charge coupled device (CCD) area-detector diffractrometer (Mo K_α graphite-monochromated radiation, λ = 0.7107 Å), equipped with an Oxford Cryosystems cryostream and controlled by the Collect software package.[27] Images were processed using the software packages Denzo and Scalepack,[28] and the data were corrected for absorption by using the empirical method employed in Sortav.[29] Structures were solved by the direct methods of SHELXS-97,[30] and refined by full-matrix least squares on F^2 using SHELXL-97.[31] All non-hydrogen atoms were directly located from difference Fourier maps and refined, when possible, with anisotropic displacement parameters. Cavity dimensions were calculated by overlapping rigid spheres with van der Waals radii for each element: O, 1.52 Å; N, 1.55 Å; C, 1.7 Å; and Cd, 2.2 Å (hydrogen atoms were omitted in all cases for simplicity).

Non-hydrogen atoms have been directly located from difference Fourier maps and refined using anisotropic displacement parameters. Hydrogen atoms attached to carbon were located at their idealized positions using HFIX instructions (43 for the aromatic and 23 for the methylene hydrogen atoms) in SHELXL,[31] and included in the refinement in riding-motion approximation with an isotropic thermal displacement parameter fixed at 1.2 times U_{eq} of the atom to which they are attached. For structures **I** and **II**, hydrogen atoms from the water molecules were also located in difference Fourier maps and refined with an isotropic displacement parameter, U_{iso}, constrained to 1.5 times U_{eq} of the parent atom. The O−H and H···H distances for these molecules were restrained to be 0.88(1) and 1.44(1) Å, respectively. These geometrical considerations are intended to provide a reasonable geometry for the water molecules. For structure **III**, the hydrogen atoms associated with the water molecules could not be directly located from difference Fourier maps, and no attempt was made to place them using geometrical considerations. However, they have been included in the empirical formula (see Table 1).

For compounds **I** and **II**, the hydrogen atoms from the protonated carboxylic acid groups were directly located from difference Fourier maps, but their position was constrained using the AFIX 83 instruction in SHELXL,[31] and an isotropic displacement parameter, U_{iso}, constrained to 1.5 times U_{eq} of the parent atom. The last difference Fourier map syntheses show the highest peaks (1.287/1.697 $eÅ^{-3}$) located at 0.21/0.36 Å from H(41)/O(3W), and the

(26) Kottke, T.; Stalke, D. *J. Appl. Cryst.* **1993**, *26*, 615.
(27) Hooft, R. Collect: Data Collection Software; Nonius B. V., Delft, 1998.
(28) Otwinowski, Z.; Minor, W. In *Methods in Enzymology*; Carter, C. W., Jr., Sweet, R. M., Eds.; Academic Press: New York, 1997; Vol. 276, p 307.
(29) Blessing, R. H. *J. Appl. Crystallogr.* **1997**, *30*, 421; Blessing, R. H. *Acta Crystallogr., Sect A: Found. Crystallogr.* **1995**, *51*, 33.
(30) Sheldrick, G. M. SHELXS-97, Program for Crystal Structure Solution; University of Göttingen, Germany, 1997.
(31) Sheldrick, G. M. SHELXL-97, Program for Crystal Structure Refinement; University of Göttingen, Germany, 1997.

deepest hole (−0.939/−1.304 $Å^{-3}$) at 0.84/0.88 Å from Cd(1), for **I**/**II**, respectively.

During the final refinement stages of structure **III**, several *Q* peaks were found, probably corresponding to highly disordered solvent molecules. From these, only three crystallization water molecules could be satisfactorily refined, with the last difference Fourier map synthesis showing the highest peak (2.831 $eÅ^{-3}$) at 1.18 Å from Cd(2), and the deepest hole (−1.306 $eÅ^{-3}$) at 0.71 Å from Cd(2).

Crystallographic data (excluding structure factors) for the structures reported in this paper have been deposited with the Cambridge Crystallographic Data Centre as supplementary publications nos. CCDC-230922 to -230924 for **I**−**III**, respectively. Copies of the data can be obtained free of charge on application to CCDC, 12 Union Road, Cambridge CB2 2EZ, U.K. [fax: (+44) 1223 336033; e-mail: deposit@ccdc.cam.ac.uk].

Acknowledgment. We are grateful to the Portuguese Foundation for Science and Technology (FCT) for financial support to F.A.A.P. through the Ph.D. scholarship No. SFRH/BD/3024/2000.

Supporting Information Available: SEM pictures of compounds **I**−**III**. Diagrams showing the crystal packing of structure **II**, along with portions of the hydrogen-bonding networks of **II** and **III**, and crystallographic information files. This material is available free of charge via the Internet at http://pubs.acs.org.

IC049523O